A Multi-Level Wave Based Method to predict the dynamic response of 2D poroelastic materials containing inclusions

Elke Deckers, Stijn Jonckheere and Wim Desmet
KU Leuven - Dept. of Mechanical Engineering, Celestijnenlaan 300B - box 2420, 3001 Heverlee (Leuven), Belgium

Summary
Poroelastic materials are often applied as effective noise measures. They are, however, most effective at higher frequencies. A lot of research has been performed to increase absorption also at lower frequencies. A promising solution is to add inhomogeneities to the foams, being inclusions or perforations. Recently, a Wave Based Method was developed to predict the dynamic response of poroelastic materials, described by the theory of Biot. This Trefftz approach was shown to be very effective for geometrically simple problems. A sufficient condition for the method to converge is that the considered problem domain is convex. Non-convex domains have to be partitioned into convex subdomains. Consequently, domains with circular inclusions cannot be accurately accounted for with the Wave Based Method; this problem was overcome with the so-called Multi-Level framework, which was introduced for acoustic and structural dynamic problems. This paper extends the Multi-Level approach to efficiently account for inclusions in a poroelastic material. The method is validated through comparison to the Finite Element Method.

PACS no. 43.20.+g

1. Introduction

Poroelastic materials are often applied as noise reduction measures in vibro-acoustic applications. As a rule of thumb the thickness of the material should at least be a quarter of the wavelength to provide good absorption, leading to bulky solutions for lower frequencies. Much research has been spent to increase the absorption in the low frequency range, without altering the thickness of the poroelastic layer. It has been shown in literature that by using e.g. perforations [1] or inclusions [2] in a foam the low-frequency acoustic properties can be drastically improved.

Poroelastic materials consist of two constituents: the elastic frame and the fluid filling the voids. Many models, applying different degrees of approximations [3, 4], are available. The theory by Biot [5], combined with the so-called Johnson-Champoux-Allard model is most commonly used to describe the coupled dynamic behaviour of the homogenised solid and fluid phases of the material, accounting for viscous, inertial and thermal effects.

The Finite Element Method (FEM) is most often used to model the fully coupled Biot equations based on different weak formulations of which the ($\mathbf{u}^s$,p)-formulation [6], with $\mathbf{u}^s$ the solid displacement vector and p the pore pressure of the poroelastic material, is preferred due to the smaller number of degrees of freedom (DOFs) per node. Although the FEM has the advantage that complex geometries can be accounted for, its use is restricted towards the low-frequency range as the computational cost increases for higher frequencies: the wavelengths are smaller and often extremely fine discretisations are needed to obtain accurate results.

Recently, the Wave Based Method (WBM) [7], a Trefftz based prediction technique has been extended to solve the Biot equations [8]. The method uses exact solutions of the governing partial differential equations to describe the field variables. Specifically for Biot models, the method explicitly accounts for the three different wave types that propagate in this class of materials. As compared to standard element based techniques, the inclusion of *a priori* known information on the physics of the problem in the model leads to a more efficient solution. The main drawback of the method is that it is limited to geometrically simple problems. A sufficient condition for the method to converge is that the considered problem domain is convex. Non-convex domains have to be partitioned into convex subdomains. Consequently, domains with

circular inclusions cannot be accurately accounted for with the WBM. To overcome this constraint, the so-called Multi-Level Wave Based Method (ML-WBM) has been introduced for acoustic and structural dynamic problems. The original problem is subdivided into 'levels' that separately account for the dynamics of the bounded domain and for the scattering of the inclusions. It combines solutions of the bounded domain and outgoing solutions exterior to the inclusions to describe the dynamic fields using the superposition principle.

This paper extends the ML-WBM approach for poroelastic materials. Unbounded wave functions are defined that are exact solutions of an unbounded poroelastic domain exterior to a circular truncation. The known bounded wave functions and novel unbounded wave functions are combined in a Multi-Level framework.

2. Problem description

The Biot theory [3] uses an equivalent solid and a compressible fluid continuum description on a macroscopic level, assuming that the pores are homogeneously distributed in the material. The two coupled partial differential equations describing the dynamic behaviour of the solid and the fluid phase are:

$$\begin{aligned} N\nabla^2\mathbf{u^s}(\mathbf{r}) + \nabla[(\lambda + \frac{\tilde{Q}^2}{\tilde{R}} + N)e^s(\mathbf{r}) + \tilde{Q}e^f(\mathbf{r})] \\ = -\omega^2(\tilde{\rho}_{11}\mathbf{u^s}(\mathbf{r}) + \tilde{\rho}_{12}\mathbf{u^f}(\mathbf{r})), \end{aligned} \quad (1)$$

$$\begin{aligned} \nabla[\tilde{Q}e^s(\mathbf{r}) + \tilde{R}e^f(\mathbf{r})] \\ = -\omega^2(\tilde{\rho}_{12}\mathbf{u^s}(\mathbf{r}) + \tilde{\rho}_{22}\mathbf{u^f}(\mathbf{r})). \end{aligned} \quad (2)$$

In these equations, $\mathbf{u}^\bullet(\mathbf{r})$ is a displacement vector, $\mathbf{e}^\bullet(\mathbf{r})$ the strain vector, $e^\bullet(\mathbf{r})$ the longitudinal strain, $\sigma^\bullet$ the stress tensor in phase $\bullet$ and λ, $\tilde{Q}$, $\tilde{R}$, $\tilde{N}$, $\tilde{\rho}_{11}$, $\tilde{\rho}_{12}$, $\tilde{\rho}_{22}$ are material properties, being fully described in literature [3, 4].

For a poroelastic material, three boundary conditions have to be specified at each point of the boundary in order to have a well-posed problem. In this paper only mechanical and mixed boundary conditions are used. The boundary $\Gamma = d\Omega$ of the considered domain Ω can be divided into two non-overlapping parts ($\Gamma = \Gamma_{ki} \bigcup \Gamma_{mi}$) along which one of the two following sets of boundary conditions hold:

- mechanical boundary conditions, where the stress resultants are prescribed:

$$\mathbf{r} \in \Gamma_{me} : \begin{cases} R_{\sigma_n^s}(\mathbf{r}) = \sigma_n^s(\mathbf{r}) - \bar{\sigma}_n^s(\mathbf{r}) = 0 \\ R_{\sigma_s^s}(\mathbf{r}) = \sigma_s^s(\mathbf{r}) - \bar{\sigma}_s^s(\mathbf{r}) = 0 \\ R_{\sigma^f}(\mathbf{r}) = \sigma_n^f(\mathbf{r}) - \bar{\sigma}^f(\mathbf{r}) = 0 \end{cases}, \quad (3)$$

  with $\bar{\sigma}_n^s(\mathbf{r})$, $\bar{\sigma}_s^s(\mathbf{r})$ and $\bar{\sigma}^f(\mathbf{r})$ the prescribed values of the normal and tangential stress resultant components of the solid phase in the normal and tangential direction to the boundary and the prescribed hydrostatic stress of the fluid phase, respectively.

- mixed boundary conditions:

$$\mathbf{r} \in \Gamma_{mi} : \begin{cases} R_{u_n^s}(\mathbf{r}) = u_n^s(\mathbf{r}) - \bar{u}_n^s(\mathbf{r}) = 0 \\ R_{u_n^f}(\mathbf{r}) = u_n^f(\mathbf{r}) - \bar{u}_n^f(\mathbf{r}) = 0 \\ R_{\sigma_s^s}(\mathbf{r}) = \sigma_s^s(\mathbf{r}) - \bar{\sigma}_s^s(\mathbf{r}) = 0 \end{cases}. \quad (4)$$

  For a sliding edge, the prescribed values of $\bar{u}_n^s(\mathbf{r})$, $\bar{u}_n^f(\mathbf{r})$ and $\bar{\sigma}_s^s(\mathbf{r})$ are zero.

3. WBM for 2-D bounded poroelastic problems

This section briefly introduces the methodology of the WBM for a general 2D poroelastic problem. A complete description can be found in [8]. The WBM is a deterministic numerical method based on an indirect Trefftz approach. It partitions the problem domain into a limited number of large convex subdomains. Convexity of the subdomains is a sufficient condition for the method to converge towards the exact solution of the problem. Within each subdomain, the dynamic field variables are approximated using an set of wave functions which intrinsically satisfy the governing Helmholtz equation(s). The DOFs are the contribution factors of each wave function in this expansion. Enforcing the boundary and interface conditions along the subdomain boundaries using a Galerkin weighted residual formulation leads to a small, complex and frequency dependent system of equations which can be solved for the contribution factor of each wave function. The general modelling procedure of the WBM consists of four steps that are briefly recalled:

1. Selection of a suitable set of wave functions for each subdomain: For sake of simplicity, this paper only considers convex subdomains.
2. Selection of suitable set of wave functions for each subdomain $\Omega^{(\alpha)}$. To apply the WB theory to poroelastic materials, the Biot equations have to be decoupled into a set of Helmholtz equations. As noted by Biot, poroelastic materials support three wave types simultaneously, one shear and two types of compressional waves. In the case that the material is isotropic, a possible decomposition for the solid displacements is given by:

$$\begin{Bmatrix} u_x^s(\mathbf{r}) \\ u_y^s(\mathbf{r}) \end{Bmatrix} = \nabla\left(-\frac{1}{k_{l_1}^2}e_1^s(\mathbf{r}) - \frac{1}{k_{l_2}^2}e_2^s(\mathbf{r})\right), \\ +\nabla\times\frac{1}{k_t^2}\omega^s(\mathbf{r}) \quad (5)$$

   with $e_1^s(\mathbf{r})$ and $e_2^s(\mathbf{r})$ two volumetric strains ($e^s(\mathbf{r}) = e_1^s(\mathbf{r}) + e_2^s(\mathbf{r})$) and $\omega^s(\mathbf{r})$ the rotational strain of the solid phase. By substituting (5) in the Biot equations (1), one obtains three decoupled Helmholtz equations with two longitudinal wave numbers k_{l_1} and k_{l_2} and one shear wave number

k_t [8]. Each of the resulting strain fields is then approximated using a set of wave functions. Each wave function $\Phi_w^{(\alpha)}$ exactly satisfies the homogeneous part of the associated decoupled Helmholtz equation. For two-dimensional bounded domains, two sets of wave functions are distinguished, the r- and the s-set:

$$\begin{cases} \Phi_{w_r}^{(\alpha)}(x,y) = \\ \qquad \left\{\sin(k_{xw_r}^{(\alpha)}x), \cos(k_{xw_r}^{(\alpha)}x)\right\} e^{-jk_{yw_r}^{(\alpha)}y} \\ \Phi_{w_s}^{(\alpha)}(x,y) = \\ \qquad e^{-jk_{xw_s}^{(\alpha)}x} \left\{\sin(k_{yw_s}^{(\alpha)}y), \cos(k_{yw_s}^{(\alpha)}y)\right\} \end{cases}, \quad (6)$$

where $\{f(x,y), g(x,y)\}\, h(x,y)$ indicates the definition of two independent basis functions $f(x,y).h(x,y)$ and $g(x,y).h(x,y)$. The following wave number components are selected to fulfill the Helmholtz equation and to ensure convergence:

$$\left(k_{xw_r}^{(\alpha)}, k_{yw_r}^{(\alpha)}\right) = \left(\frac{w_1^{(\alpha)}\pi}{L_x^{(\alpha)}}, \pm\sqrt{k_j^2 - \left(k_{xw_r}^{(\alpha)}\right)^2}\right), \quad (7)$$

$$\left(k_{xw_s}^{(\alpha)}, k_{yw_s}^{(\alpha)}\right) = \left(\pm\sqrt{k_j^2 - \left(k_{yw_s}^{(\alpha)}\right)^2}, \frac{w_2^{(\alpha)}\pi}{L_y^{(\alpha)}}\right), \quad (8)$$

with $w_1^{(\alpha)} = 0, 1, 2, \ldots$ and $w_2^{(\alpha)} = 0, 1, 2, \ldots$ The dimensions $L_x^{(\alpha)}$ and $L_y^{(\alpha)}$ are the dimensions of the (preferably smallest) bounding rectangle circumscribing the considered subdomain and k_j is the physical wave number of the considered Helmholtz equation.

3. Construction of the WB system matrices via a weighted residual formulation of the boundary and interface conditions. Following a Galerkin approach, the weighting functions are expanded using the same wave functions as applied for the field variables.
4. Solution of the system of equations, yielding the wave function contribution factors and postprocessing of the dynamic variables.

4. Multi-Level WBM for poroelastic problems

Dynamic problems containing scatterers or inclusions are difficult or impossible to model using the standard WBM due to the convexity requirement. To overcome this problem, the ML concept has been developed. The ML approach was in a first step developed for unbounded acoustic multiple scattering configurations [9] and was afterwards extended towards bounded problems [10]. It subdivides the problem into different 'levels'; each level accounts for the dynamic field of only the bounded problem domain without inclusions or of the scattering of one single inclusion. The total solution field can then be obtained by combining the different levels of the problem, using the superposition principle. The concept is illustrated in Figure 1, showing a bounded problem domain with two inclusions. For the sake of simplicity, only circular inclusions are considered. The multi-level WBM approach consists of four steps and are briefly revisited and then applied to poroelastic problems:

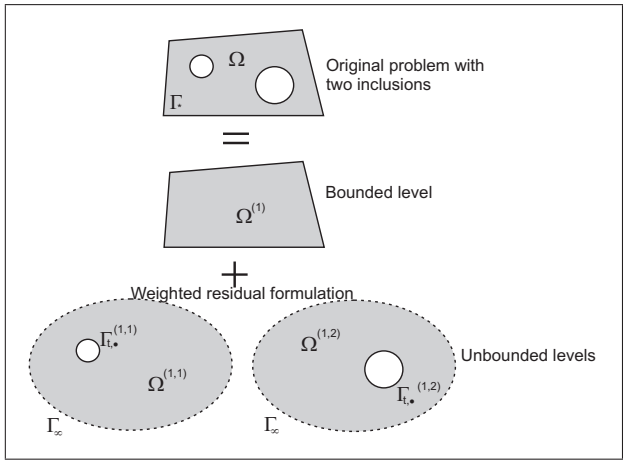

Figure 1. Illustration of the WBM Multi-Level concept.

1. *Division of the original problem into levels:*
   In a first step the problem is divided into a number of levels: The first level includes the bounded problem as if there were no inclusions present. If needed, this bounded domain can be subdivided into non-overlapping convex subdomains $\Omega^{(\alpha)}$ where α indicates the index of the bounded subdomain. In this paper, only one bounded subdomain $\Omega^{(1)}$ is considered. Each other level contains one single inclusion as if the bounded domain and the other inclusions were not present. The region exterior to the scatterer within an unbounded level is truncated by a truncation circle $\Gamma_{t,\bullet}^{(\alpha,\beta)}$ where α indicates the index of bounded subdomain to which to inclusion belongs and β indicates the index of the unbounded level. The truncation circle subdivides the region exterior to the inclusion in bounded and unbounded domains. In this paper, the truncation circle coincides with the boundary of the inclusion, such that only an unbounded submain results. The truncation surface $\Gamma_{t,\bullet}^{(\alpha,\beta)}$ can be subdived into different zones, indicated with subscript $\bullet$, on which different boundary or interface conditions are imposed. In this paper, only sliding edge conditions (4) are considered. The unbounded region exterior to $\Gamma_{t,\bullet}^{(\alpha\beta)}$ is denoted $\Omega^{(\alpha,\beta)}$. The problem depicted in Figure 1 is thus divided into three levels: One bounded level consisting of only one bounded subdomain $\Omega^{(1)}$, and two unbounded levels each containing one unbounded subdomain, $\Omega^{(1,1)}$ and $\Omega^{(1,2)}$.
2. *Selection of wave functions for the different levels:*
   For each level, a suitable wave function set is se-

lected. For the bounded domain $\Omega^{(1)}$, resulting from the bounded level, poroelastic wave functions are selected based on the smallest bounding box circumscribing the bounded subdomain as described in the previous section. For the unbounded levels, poroelastic wave functions are needed that describe the dynamic poroelastic fields exterior to the associated truncation circle. These wave functions should *a priori* fulfill the radiation conditions at the boundary at infinity Γ_∞. The well-known Kupradze radiation conditions for radiated P- and S-waves are applied [11]. Besides, of course, all wave functions should inherently fulfill one of the decoupled Helmholtz equations. The following unbounded wave functions are selected for subdomains $\Omega^{(1,\beta)}$

$$\Psi_{l_\star}^{(\beta)}(r,\theta) = \begin{cases} H_v^{(2)}(k_{l_\star} r)\cos(v\theta), & v = 0,1,\dots \\ H_v^{(2)}(k_{l_\star} r)\sin(v\theta), & v = 1,2,\dots \end{cases}, \tag{9}$$

$$\Psi_{t}^{(\beta)}(r,\theta) = \begin{cases} H_v^{(2)}(k_{t} r)\cos(v\theta), & v = 0,1,\dots \\ H_v^{(2)}(k_{t} r)\sin(v\theta), & v = 1,2,\dots \end{cases}, \tag{10}$$

where $\star$ is 1 or 2. Once the field variables for the different levels have been defined, they are combined for the common domain Ω by using the superposition principle. Let us denote $\hat{\chi}^{(1)}(\mathbf{r})$ the considered field variable approximation of the bounded poroelastic subdomain $\Omega^{(1)}$ and $\hat{\chi}^{(1,\beta)}(\mathbf{r})$ the field variable approximation of the β-th unbounded poroelastic subdomain $\Omega^{(1,\beta)}$. Then the dynamic field $\hat{\chi}^{(1')}(\mathbf{r})$ in $\Omega^{(1')}$=$\Omega^{(1)} \bigcap \Omega^{(1,1)} \bigcap \Omega^{(1,2)}$ can be written as:

$$\hat{\chi}^{(1')}(\mathbf{r}) = \hat{\chi}^{(1)}(\mathbf{r}) + \hat{\chi}^{(1,1)}(\mathbf{r}) + \hat{\chi}^{(1,2)}(\mathbf{r}). \tag{11}$$

3. *Construction of the system of equations:*
The boundary and interface conditions need to be enforced, which is again achieved by using a weighted Galerkin scheme, using the compound wave function sets for subdomains $\Omega^{(1')}$. The choice of weighting function is different for the different boundaries. To have valid weighting functions, they have to be able to represent the dynamic field on the considered boundary. Consequently the unbounded wave functions associated with a certain truncation surface are used as weighting functions for the residuals on that truncation and the bounded wave functions are used as weighting functions on the exterior boundaries of the domain.
4. *Solution and post-processing:*
The system matrices can be solved for the unknown contribution factor of all wave functions. In a post-processing step the response field can be evaluated in which the variable expansion of $\Omega^{(1')}$ is used.

A more detailed description can be found in [10] for acoustic and plate membrane problems.

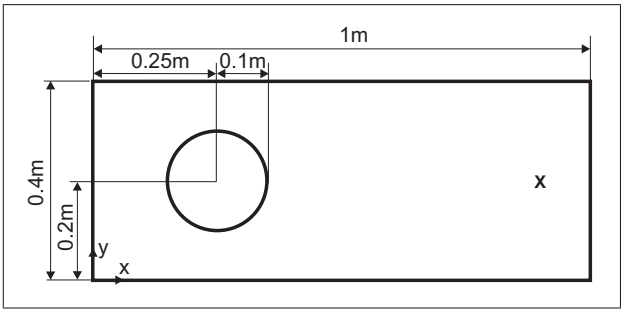

Figure 2. Rectangular poroelastic domain with a circular inclusion, x indicates the postprocessing point in which frequency response functions are calculated.

5. Numerical verification example

Figure 2 shows the problem geometry used to validate the ML-WBM implementation for the poroelastic Biot equations. A rectangular domain of 1m by 0.4m is considered, containing one inclusion of radius 0.1m. On the top layer an acoustic pressure $p^a(x) = x^3 - 2x^2 + 1$ N/m^2 excites the system. On all other boundaries sliding edge conditions (4) are imposed. The considered poroelastic material is a polurethane foam; its properties and those of the saturating air are given in Table I.

Air properties	
Thermal conductivity	$k = 2.57 \cdot 10^{-2} W(mK)$
Specific heat	$c_p = 1.005 \cdot 10^3 J/(kgK)$
Gas constant	$R = 286.7 m^2/(s^2 K)$
Temperature	$T = 293.15K$
Ratio of specific heats	$\gamma = 1.4$
Fluid kinematic viscosity	$\nu_f = 15.11 \cdot 10^{-6} m^2/s$
Fluid density	$\rho_f = 1.205 kg/m^3$
Polyurethane foam material	
Young's modulus	$E_s = 70 \cdot 10^3 Pa$
Loss factor	$\eta_l = 0.15$
Poisson ratio	$\nu = 0.39$
Bulk density of the solid phase	$\rho_1 = 22.1 kg/m^3$
Porosity	$h = 0.98$
Viscous characteristic length	$\Lambda = 1.1 \cdot 10^{-4} m$
Thermal characteristic length	$\Lambda' = 7.42 \cdot 10^{-4} m$
Static flow resistivity	$\sigma = 3.75 \cdot 10^3 kg/(m^3 s)$
Tortuosity	$\alpha_\infty = 1.17$

Table I. Material properties of air and polyurethane foam

To benchmark the WB results, different FE models, based on the (u,p)-formulation [6], are implemented in Comsol 4.4a using quadratic triangular Lagrangian elements. The WBM code is implemented in Matlab R2013b. All calculations are run on a Linux-based 2.8 GHz Ivy bridge system with 64GB RAM. Convergence studies are run single threaded.

Figure 3 shows the contour plot of the absolute value of the solid displacement in the x-direction, $|u_x^s|$, calculated with the WBM at 500Hz. In total 555 wave functions are used: 492 bounded and 63 unbounded wave functions. These numbers are selected such that the smallest wavelength resulting in the wave functions is less or equal to the smallest physical wave-

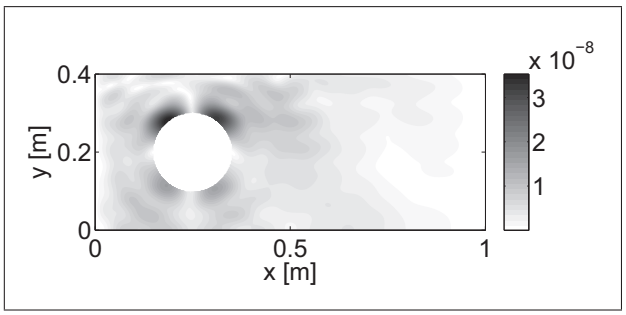

Figure 3. Contour plot of $|u_x^s|$ at 500Hz, calculated with WBM (555 DOFs).

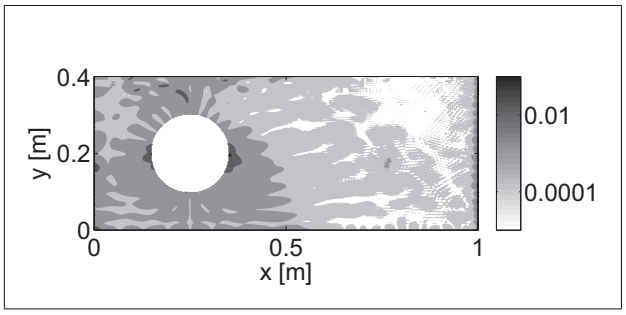

Figure 4. Logarithmic relative error $\varepsilon(\hat{u}_x^s(\mathbf{r}))$ of the WBM model (555 DOFs) with respect to FEM (454,815 DOFs).

length at the considered frequency. For the three different wave types, the same number of wave functions is applied. The figure clearly shows that the imposed boundary conditions on the left and right hand side are fulfilled. Figure 4 shows the logarithm of the relative error with respect to a fine FE model, calculated as:

$$\varepsilon(\hat{u}_x^s(\mathbf{r})) = \frac{|\hat{u}_x^s(\mathbf{r}) - u_{x_{ref}}^s(\mathbf{r})|}{|u_{x_{ref}}^s(\mathbf{r})|}. \tag{12}$$

The reference FE model was constructed by starting from a coarse FE mesh of 378 DOFs and running 11 adaptive refinements such that a model of 454,815 DOFs is obtained. A good accuracy is seen, except for zones where the displacement is close to zero and the relative error is most sensitive to small variations due to a division by nearly zero.

Figure 5 shows the real and imaginary part of the shear stress σ_{xy}^s of the solid phase, evaluated in a point with coordinates (0.9,0.2), with the WBM and the FEM. For the FEM, again 11 adaptive refinements are used for each frequency line. The number of wave functions is increased with frequency according to the same rule. The results are on top of each other, showing that accurate results are obtained for the frequency range of interest.

Finally, a convergence study has been performed to assess the potential of the ML-WBM with respect to the FEM for poroelastic materials. Two different frequencies are considered: 250Hz and 750Hz. The aver-

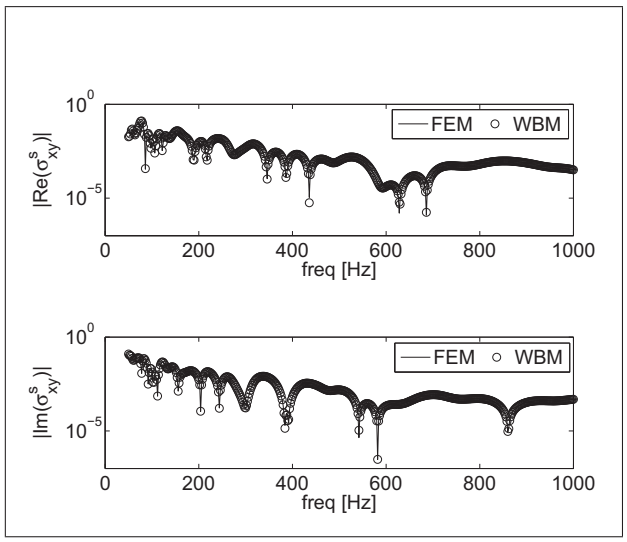

Figure 5. Frequency response function of the shear stress of the solid phase σ_{xy}^s evaluated in point (0.9,0.2) and calculated with the WBM and FEM.

Model number	♯ DOFs	h_{max} [m]
1	1,302	0.1
2	2,664	0.067
3	3,354	0.053
4	5,076	0.037
5	15,876	0.02
6	60,312	0.01
7	239,184	0.005
8	952,608	0.0025
9	3,802,176	0.00125

Table II. FEM model data

age relative prediction error on the pore pressure is calculated according to:

$$\varepsilon = \frac{1}{n}\sum_{j=1}^{n}\varepsilon_j \quad \text{with} \quad \epsilon_j = |\frac{\hat{p}^f(\mathbf{r_j}) - p^{f^{ref}}(\mathbf{r_j})}{p^{f^{ref}}(\mathbf{r_j})}|. \tag{13}$$

with n the number of selected response point. For this specific case 14 equally distributed response points are chosen in the problem domain. Table II contains the FEM model information. These models are regularly refined, to avoid the overhead cost related to subsequent adaptive refinements. The number of wave functions is increased from 45 to 1137 at 250Hz and from 123 to 3357 at 750 Hz applying minimal wavelengths corresponding to 0.1 to 4 times the minimal physical wavelength. An adaptively refined quadratic FE model is used as a reference, starting from a coarse 378 DOFs model and applying 13 adaptive refinements such that models of 2,528,712 DOFs and 1,732,341 DOFs are obtained at 250 and 750Hz, respectively.

Figure 6 shows the convergence curves at 250Hz (black) and 750 (grey) obtained using the WBM and the FEM. It is clear that the WBM profits from an increased efficiency by embedding known physical information on the solution field. It is also seen that the WBM convergence curves stagnate at the accuracy of the reference model. When frequency increases, the same number of FEM DOFs leads to a lower accuracy for the same calculation time.

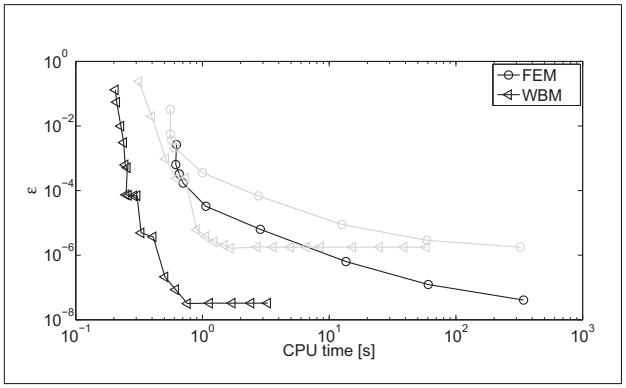

Figure 6. Convergence curves of the pore pressure at 250 (black) en 750 (grey) Hz. Finest adaptive FE model used as a reference.

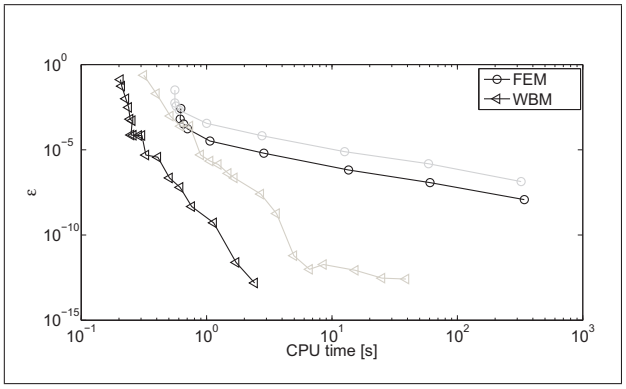

Figure 7. Convergence curves of the pore pressure at 250 (black) en 750 (grey) Hz. Finest WBM model used as a reference.

To illustrate the efficiency of the WBM, the finest WBM model is taken as a reference in Figure 7, showing that the solution keeps on converging at a high rate. Excellent accuracies are obtained in a very short calculation time.

6. CONCLUSIONS

In recent work, the WBM has been extended to poroelastic problems, described by the Biot equations. Though very promising results have been obtained for simple geometries, the method is hampered by its convexity requirement: domains containing inclusions cannot be efficiently modelled. For acoustic and dynamic plate problems the so-called multi-level framework was introduced. This framework subdivides the problem domain in levels; each level considers the dynamic response of only the bounded domain without inclusions or the scattering due to a single inclusion. This paper extends the Multi-Level WBM framework for poroelastic materials: unbounded wave functions are derived and combined with bounded wave functions through superposition principle. The method is evaluated against standard FEM models based on the ($\mathbf{u}^s$,p)-formulation. The potential of the method is illustrated by a numerical verification example.

Acknowledgement

Elke Deckers is a Postdoctoral Fellow of the Fund for Scientific Research - Flanders (F.W.O.-Vlaanderen), Belgium. The Research Fund KU Leuven is gratefully acknowledged for its support.

References

[1] F.C. Sgard, X. Olny, N. Atalla and F. Castel: On the use of perforations to improve the sound absorption of porous materials. Applied Acoustics 66 (2005) 625-651.

[2] E. Gourdon and M. Seppi: On the use of porous inclusions to improve the acoustical response of porous material: Analytical model and experimental verification. Applied Acoustics 71 (2010) 283-298.

[3] J.F. Allard, N. Atalla: Propagation of Sound in Porous Media: Modeling Sound Absorbing Materials. John Wiley & Sons, West Sussex, United Kingdom, 2009.

[4] E. Deckers, S. Jonckheere, D. Vandepitte and W. Desmet: Modelling Techniques for Vibro-Acoustic Dynamics of Poroelastic Materials. Archives of Computational Methods in Enineering (2014), DOI10.1007/s11831-014-9121-0.

[5] M. A. Biot: The theory of propagation of elastic waves in a fluid-saturated porous solid. I. Low frequency range. II. Higher frequency range. Journal of the Acoustical Society of America 28 (1956) 168-191.

[6] N. Atalla, R. Panneton, P. Debergue: Enhanced weak integral formulation for the mixed ($\underline{u}$,$\underline{p}$) poroelastic equations. Journal of the Acoustical Society of America 109 (2001) 3065-3068.

[7] E. Deckers, O. Atak, L. Coox, R. D'Amico, H. Devriendt, S. Jonckheere, K. Koo, B. Pluymers, D. Vandepitte and W. Desmet: The Wave Based Method: an overview of 15 years of research. Wave Motion 51 (2014) 550-565.

[8] E. Deckers, N.-E. Hörlin, D. Vandepitte and W. Desmet: A Wave Based Method for the efficient solution of the 2D poroelastic Biot equations. Computer Methods in Applied Mechanics and Engineering 201-204 (2012) 245-262.

[9] B. Van Genechten, B. Bergen, D. Vandepitte and W. Desmet: A Trefftz-based numerical modelling framework for Helmholtz problems with complex multiple scatterer configurations. Journal of Computational Physics 229 (2010) 6623-6643.

[10] B. Van Genechten, K. Vergote, D. Vandepitte and W. Desmet: A Multi-Level Wave Based numerical modelling framework for the steady-state dynamic analysis of bounded Helmholtz problems with multiple inclusions. Computer Methods in Applied Mechanics and Engineering 199 (2010) 1881-1905.

[11] P. Martin: Multiple Scattering, Interaction of Time-Harmonic Waves with N obstacles, vol. 107 of Encyclopedia of Mathematics and its Applications. Cambridge university Press, 2006.